Shape and Composition Map of a Prepyramid Quantum Dot

B. J. Spencer and M. Blanariu

Department of Mathematics, State University of New York at Buffalo, Buffalo, New York 14260-2900, USA

(Received 3 January 2005; published 10 November 2005)

We present a theory for the shape, size, and nonuniform composition profile of a small prepyramid island in an alloy epitaxial film when surface diffusion is much faster than deposition and bulk diffusion. The predicted composition profile has segregation of the larger misfit component to the island peak, with segregation enhanced by misfit strain and solute strain but retarded by alloy solution thermodynamics. Vertical composition gradients through the center of the island due to this mechanism are on the order of 2%/nm for Ge_XSi_{1-X}/Si and 10–15%/nm for $In_XGa_{1-X}As/GaAs$.

DOI: 10.1103/PhysRevLett.95.206101 PACS numbers: 68.55.−a, 61.46.+w, 68.35.−p, 68.65.−k

The self-assembly of quantum dots (QDs) has received considerable attention as a means of fabricating structures for optoelectronic applications. A substantial amount of theoretical work exists (for a review see Ref. [1]), but essentially all of it neglects the important influence of alloying. The principal difficulty in understanding alloy QD formation is a complicated interdependence of QD shape, strain and composition. While there have been experimental investigations of alloy quantum dots [2–17], a recent literature review [18] suggests that no existing theory can predict QD size, shape, and composition. Of the theoretical work, Tersoff [19] has discussed the nucleation of faceted pyramids of uniform composition, and the possible formation of compositional nonuniformity. Liu *et al.* [2] described an ''inverse triangle'' segregation pattern in a two-dimensional island of assumed triangular shape.

In this Letter, we present a quantitative theory for the shape and composition profile of small ''prepyramid'' islands. We focus here on conditions for which surface diffusion is much faster than deposition, with bulk diffusion being negligible, as in Ref. [2]. This describes a growth scenario wherein a small amount of material is deposited per unit time, and this material has time to diffuse over the island surface to its equilibrium configuration before new material is deposited. As growth occurs, the buried surface layers become the interior of the island. Thus, the entire problem consists of determining a sequence of equilibrium surfaces of nonuniform composition as the dot grows. The more general problem involves interdiffusion of the substrate into the island and wetting layer, as well as the competition between deposition and the dynamics of surface diffusion, leading to surfaces being buried before reaching equilibrium. Later we address the conditions for which our simplified theory is an accurate model for these dynamics.

Figure 1 illustrates the main results of our theory for an axisymmetric, isotropic prepyramid island. The shape of the island is determined by the equilibration of surface chemical potentials for each alloy component. The nonuniform stress due to the island shape causes nonuniform composition along the island surface with the larger misfit component segregating to the island peak. As the island grows these nonuniform surface compositions are buried to create a nonuniform composition profile within the island as shown in Fig. 1. Our theoretical results provide explicit formulas for the shape, size, and composition map in the island. The results are restricted to small unfaceted prepyramid islands [20]; nonetheless, the results provide a concrete benchmark for analyzing the development of compositional nonuniformity in quantum dots.

The theoretical model is as follows. We consider a single axisymmetric island and make a simplifying assumption of isotropic material properties. We take the substrate surface to lie in $z < 0$ with the island surface $z = h(r)$ for $0 \le r \le R$ and the wetting layer $h(r) = 0$ for $r > R$, with edge conditions $h'(0) = 0$, $h(R) = 0$, and $h'(R) = 0$ [21]. This corresponds to the ''glued wetting layer'' model [22] in which a wetting layer of negligible thickness covers the substrate at $z = 0$. We take the film to be a binary alloy of components A and B with compositions C_A and C_B (with

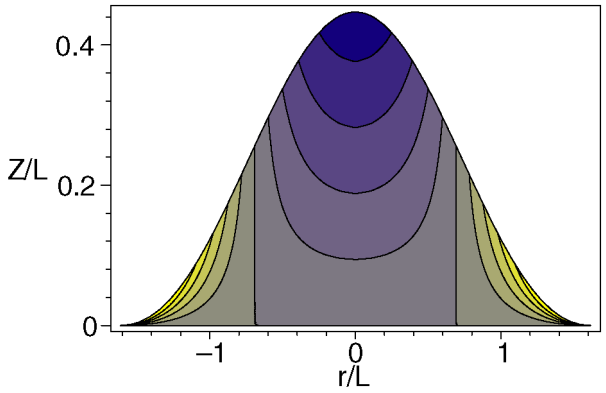

FIG. 1 (color online). Island shape and composition map. The scaled island shape is $H_0(r)/L$. The composition map is a contour plot of C_B^1/C, the scaled deviation from the reference composition. The step between contours is 0.25, vertical lines are the zero contours, and dark corresponds to negative values. Results are for $\nu = 0.276$.

$C_A + C_B = 1$). The composition profile in the island is $C_B(r, z)$. Figure 1 illustrates the island geometry and nonuniform composition profile.

The continuum model for the growth of strained alloy films has been derived in Ref. [23]. Here we seek equilibrium solutions to these dynamic equations which correspond to surface equilibrium, i.e., surface morphology and surface compositions corresponding to constant chemical potentials. For the island geometry we seek island shapes $z = h(r)$ which correspond to a prescribed volume V, and the composition profile $C_B(r, z)$ which conserves the average island composition C_B^0,

$$V = 2\pi \int_0^R h(r) r dr, \tag{1}$$

$$2\pi \int_0^R \int_0^{h(r)} C_B(r, z) r dz dr = C_B^0 V. \tag{2}$$

Hooke's law for stress T_{ij} in the film (F) is in terms of an effective strain tensor E_{ij}, where E_{ij} is the sum of gradients of the displacement u_i and a compositional strain proportional to the solute expansion coefficient η:

$$T_{ij} = \frac{E}{1+\nu}\left[E_{ij} + \frac{\nu}{1-2\nu} E_{kk}\delta_{ij} \right], \tag{3}$$

$$E_{ij} = (1/2)(u_{i,j} + u_{j,i}) - \eta(C_B - C_B^0)\delta_{ij}. \tag{4}$$

The constitutive law for stress in the substrate (S) is given by Eqs. (3) and (4) with the compositional strain explicitly zero. Mechanical equilibrium inside the film and substrate require that the stress tensors in the film and substrate be divergence-free ($\partial_i T_{ij} = 0$), with the boundary conditions: (i) traction-free film surface with normal n_j ($T_{ij}^F n_j = 0$), (ii) force balance at the film or substrate interface ($T_{3j}^F = T_{3j}^S$), (iii) jump condition on the displacement at the film or substrate interface proportional to biaxial misfit strain ϵ ($\underline{u}^F = \underline{u}^S + \epsilon[x, y, 0]$), and (iv) displacements in the substrate decay to zero far away ($\underline{u}^S \to 0$). Finally, Eqs. (5) and (6) are the chemical potentials (per volume) for each component on the island surface [23], where μ_B^c, μ_A^c are the chemical potentials from bulk alloy thermodynamics in the absence of stress, γ is the surface energy and κ is the surface curvature. Equation (7) gives the regular solution model for component $i = A, B$ where G_i is the Gibbs energy of component i per volume, K is the Boltzmann constant (per volume), and Ω is the regular solution interaction parameter:

$$\mu_A = \mu_A^c + \frac{1}{2} T_{kl} E_{kl} + \gamma\kappa + C_B \eta T_{kk}, \tag{5}$$

$$\mu_B = \mu_B^c + \frac{1}{2} T_{kl} E_{kl} + \gamma\kappa - C_A \eta T_{kk}, \tag{6}$$

$$\mu_i^c = G_i + KT \ln C_i + \Omega(1 - C_i)^2. \tag{7}$$

As simplifying approximations, we assume that the film properties such as surface energy γ, Young's modulus E, and Poisson's ratio ν are independent of the small composition variations that arise, and we also take the elastic constants in the film and substrate to be equal.

Equilibrium island shapes are solutions to Eqs. (1)–(7), corresponding to constant chemical potentials μ_A and μ_B on the island surface for given volume V and composition C_B^0. The unknowns are the island shape $h(r)$, composition profile of the island $C_B(r, z)$, displacement vectors $u_i^F(x, y, z)$ and $u_i^S(x, y, z)$, and also R, μ_A, and μ_B. We obtain closed-form solutions in the case of a small "thin" island, with the island height much smaller than its width. The typical length scale for lateral features is $L = \gamma/\sigma\epsilon$ where $\sigma = \epsilon E/(1 - \nu)$ is the biaxial misfit stress. We thus define a small parameter $\delta = V/L^3 \ll 1$ measuring the nondimensional volume of the thin island, introduce the scaled island shape $H(r) = h(r)/\delta$ and the "thin film" scale $z = \delta Z$ in the film only, and seek small-δ expansions for the island shape $[H(r) = H_0(r) + \cdots]$, composition $[C_B(r, z) = C_B^0 + \delta C_B^1(r, Z) + \cdots]$, island radius $(R = R_0 + \cdots)$, as well as the displacements and chemical potentials.

We give here the key results and their interpretation in view of experiments; details of the asymptotic analysis can be found in Ref. [24]. At order δ Eqs. (5) and (6) give a pair of coupled integrodifferential equations for the island shape and surface composition. These equations can be combined to give a single equation for the shape. This single equation can be related directly to the analogous small-slope theory for a nonalloy island [21] in which the island size appears as an eigenvalue and the solution can be constructed in terms of a Bessel series. The island shape in the alloy problem is then found to be

$$H_0(r) = A\left[a_0 + \sum_{j=1}^{\infty} a_j J_0\left(\frac{z_j r}{R_0}\right) \right] \tag{8}$$

where the island size is $R_0 = 2.061L/(1 + \nu)$, with $A = 0.462(1 + \nu)^2 L$, $a_0 = 0.162$, $a_1 = 0.419$, $a_2 = 0.0160$, $a_3 = -0.003\,99$, $a_4 = 0.001\,59$, and z_j is the jth zero of $J_1(z)$. From this known shape, the surface and interior compositions can be constructed from the surface equilibrium conditions to give

$$C_B^1(r, Z) = C\left[\alpha + \frac{L}{r}\frac{d}{dr}\left(r\frac{dH_0}{dr} \right) \right]\frac{Z}{H_0(r)}, \tag{9}$$

$$C = \frac{\epsilon\eta}{2\eta^2 + g(1-\nu)/E}, \tag{10}$$

$$g = \frac{KT}{C_A^0 C_B^0} - 2\Omega, \tag{11}$$

where $\alpha = 0.281(1 + \nu)^4$. Here C is an important scale factor which sets the magnitude of the composition variations, while g is the second derivative of the Gibbs free energy with respect to composition.

Thus, as with the case of a small isotropic island in a single-component film, the shape and size of an alloy island depends only on the length scale L and ν. In this

limit of small-island volume, the width is fixed, and the island height scales with the island volume. Figure 1 illustrates the island shape $H_0(r)$. Figure 1 also shows the composition profile C_B^1/C. The sign of the composition segregation depends on the sign of C. Typically $g > 0$, so the sign of C is given by the sign of $\eta\epsilon$, which means that the larger misfit component segregates to the island peak; i.e., Ge segregates to peaks of GeSi islands on Si.

In original dimensional variables the island shape is $z = h(r) \approx (h_*/H_*)H_0(r)$ where h_* is the actual height of the island and $H_* = 0.275L(1+\nu)^2$. In the small-island limit, the radius $R \approx R_0$ remains fixed, and the height scales linearly with the island volume $V \approx L^3 h_*/H_*$. Similarly, the composition profile in the island is $C_B(r,z) \approx C_B^0 + (h_* z/H_* h(r))C_B^\Sigma(r)$, where $C_B^\Sigma(r)$ is the surface composition in Eq. (9). A useful measure of the compositional segregation is the composition along the island center line $r = 0$:

$$C_B(0,z) \approx C_B^0 + \mathcal{G}z \tag{12}$$

where $\mathcal{G} = C_B^\Sigma(0)/H_*$ is the vertical composition gradient along the island center line.

To illustrate our results, we consider Ge_XSi_{1-X} films on a Si substrate, where X is the nominal "as-deposited" composition. Our theory predicts that the radius of a small island is $R \approx 2.061L/(1+\nu)$. In Fig. 2 we compare our theory to observations of the smallest observed prepyramid islands from a wide range of growth conditions. There is good agreement over two magnitudes of variation in the island size.

Figure 3 shows how the center-line gradient $\mathcal{G}$ varies for different film or substrate systems. The magnitude of segregation is set by C, which increases with larger misfit ϵ (e.g., $X = 1$ for Ge_XSi_{1-X} on Si). On the other hand, segregation is enhanced when g is small, e.g., $X = 0.5$ for a regular solution model. Thus, maximum segregation occurs at an intermediate composition $0.5 < X < 1$ which represents a compromise between the driving force due to misfit strain and the restoring force of solution thermodynamics. This behavior is evidenced in Fig. 3 for Ge_XSi_{1-X} on Si and $In_XGa_{1-X}As$ on GaAs. The competition of strain and alloy thermodynamics means that segregation is in general promoted at lower temperatures and in systems with large $|\eta|$ and large solute interaction parameter Ω, also illustrated in Fig. 3. In both systems, lower temperature promotes segregation, however, the magnitude is quite different for each system, 2%/nm for GeSi versus 10–15%/nm for InGaAs, because η and Ω are significantly larger for InGaAs.

While our theory is similar in spirit to Ref. [2] in that it predicts segregation of the larger misfit component to the island peak, the details are different. The main difference is that in [2] the island shape is prescribed *a priori* to remain a fixed triangular (faceted) shape as the island grows, while we determine the arbitrary (nonfaceted) island shape from the conditions for surface equilibrium. Another difference is that in [2] the surface compositions are assumed to be proportional to the elastic stresses at the surface, while we obtain a more complicated interdependence of the surface compositions on the surface shape and stress. The effect of these different assumptions is that the predicted composition profiles are only qualitatively similar. While both models predict segregation of the larger misfit component to the island peak, in [2] the composition within the island depends only on the angular position with respect to the center of the island base; hence there is no vertical concentration gradient along the island center line, in contrast to the composition map we find in Fig. 1. In addition, the use of a faceted island shape in [2] with other approximations results in weak singularities in the composition at island corners; our theory applies only to nonfaceted islands, but gives nonsingular compositions.

To our knowledge there have not been measurements of composition profiles in small prepyramid islands, but rather in larger "pyramid" or "dome" islands. While our theory is not appropriate for the description of large

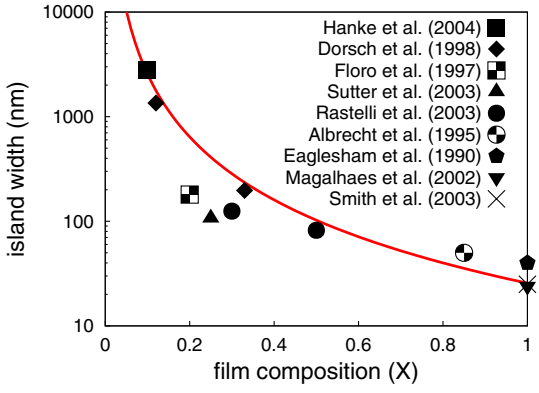

FIG. 2 (color online). Island width for Ge_XSi_{1-X} on Si. The misfit is $\epsilon = -\eta X$ and parameters used for GeSi are $\eta = 0.042$, $\nu = 0.276$, $E = 11.6 \times 10^{11}$ erg/cm^3, $\gamma = 2220$ erg/cm^2. Data from Refs. [9,13,17,26–31].

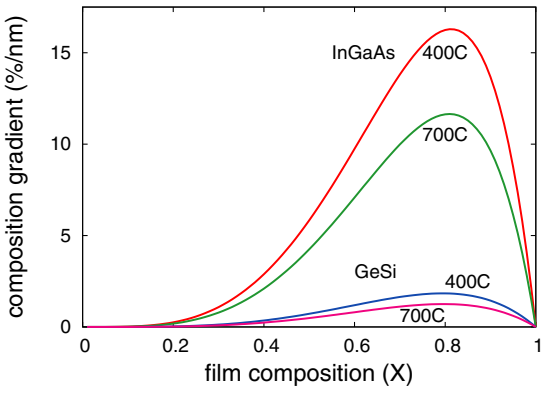

FIG. 3 (color online). Vertical composition gradient $\mathcal{G}$ along the island center line for GeSi/Si and InGaAs/GaAs. For GeSi/Si, $\Omega = 3.47 \times 10^9$ erg/cm^3; for InGaAs/GaAs, $\eta = 0.069$, $\nu = 0.332$, $E = 6.82 \times 10^{11}$ erg/cm^3, $\gamma = 1650$ erg/cm^2, and $\Omega = 4.12 \times 10^9$ erg/cm^3.

islands, it does give qualitative agreement with the general trend of preferential segregation of the larger misfit component to the island peak that has been observed in GeSi/Si [15,16] and InGaAs/GaAs [2,10].

A critical assumption in our theory is that bulk diffusion is much smaller than deposition. This requires the diffusion flux from the substrate into the wetting layer to be small relative to the deposition flux. Based on dimensional analysis, the condition for neglecting bulk diffusion is $D_B/\delta_w \ll R$. where D_B is the bulk diffusivity (cm^2/s), δ_w is the wetting layer thickness, and R is the deposition rate (cm/s). For Ge/Si growth, $\delta_w = 3$ ML and $R = 1.4$ ML/min [8] gives bulk diffusion as being negligible when $D_B \ll 10^{-17}$ cm^2/s. Such a condition should easily be satisfied at low to moderate temperatures. For example, in the experiments of Ref. [8], bulk interdiffusion was neglible for Ge/Si at 400 °C and $R = 1.4$ ML/min; in Ref. [6], bulk diffusion was negligible up to 550 °C with a faster deposition rate of $R = 10$–20 ML/min.

The second mass transport assumption is that surface diffusion is much faster than deposition. Surface diffusion is ''fast'' if the time scale for the formation of islands is small relative to the time to deposit the wetting layer. An estimate of the time scale for the formation of islands is the time scale for the stress-driven morphological instability for a single-component film [25], $t_{\mathrm{instab}} \approx L^4 KT/D_S a\gamma$ where D_S is the surface diffusivity and a is the thickness of a monolayer. Since the time to deposit the wetting layer is $t_{\mathrm{dep}} = \delta_w/R$, an estimate of the conditions for which surface diffusion dominates is $t_{\mathrm{instab}} \ll t_{\mathrm{dep}}$. Based on the results in Ref. [25], for Ge on Si this criteria is satisfied when $D_S \gg 10^{-12}$ cm^2/s, which corresponds to $T \geq 330$ °C. Thus, for Ge/Si our assumptions would appear to be reasonable for temperatures from roughly 330 °C up to about 400–550 °C depending on the deposition rate, with the assumption of negligible bulk diffusion failing at higher temperatures.

When bulk diffusion is not negligible, e.g., high temperatures [12] and low growth rates [7], an important feature of island growth is the intermixing of the substrate and island [3–9] causing large composition gradients across the film or substrate interface. Measurements of the composition near the film or substrate interface show this composition gradient to be on the order of 15%/nm for Ge/Si [8] in a case where intermixing is strong. Our predictions of the composition gradients for Ge/Si (Fig. 3) due to surface diffusion alone are *at most* 2%/nm, which suggests that the segregation mechanism we describe becomes less significant than the bulk diffusion mechanism at high temperatures and low growth rates.

Another effect of bulk diffusion is that intermixing in the wetting layer leads to islands with composition different than that of the as-deposited film [8]. The determination of the effective composition of the island due to intermixing in the wetting layer would necessarily require a more detailed model which includes bulk diffusion. However, since our theory only requires that the surface diffusion flux feeding island growth remains constant in composition, it could be adapted to the case where intermixing in the wetting layer produces an island with a different average composition than the as-deposited film. In this case C_B^0 would be interpreted as the (assumed constant) composition of the wetting layer from which the islands form. While our theory is not able to predict this composition of the wetting layer, it can still give useful benchmarks on the magnitude of compositional segregation in the case when the average composition of the island is different from the as-deposited composition (e.g., interpret X as the average island composition in Fig. 3).

This work is supported by an NSF Nanoscale Interdisciplinary Research Team Grant No. DMR-0102794. We gratefully acknowledge discussions with Peter Voorhees.

[1] V. A. Shchukin and D. Bimberg, Rev. Mod. Phys. **71**, 1125 (1999).
[2] N. Liu *et al.*, Phys. Rev. Lett. **84**, 334 (2000).
[3] S. A. Chaparro *et al.*, Phys. Rev. Lett. **83**, 1199 (1999).
[4] X. Z. Liao *et al.*, Phys. Rev. B **60**, 15 605 (1999).
[5] X. Z. Liao *et al.*, Appl. Phys. Lett. **77**, 1304 (2000).
[6] M. DeSeta *et al.*, J. Appl. Phys. **92**, 614 (2002).
[7] Y. Zhang *et al.*, Appl. Phys. Lett. **80**, 3623 (2002).
[8] M. Floyd *et al.*, Appl. Phys. Lett. **82**, 1473 (2003).
[9] D. J. Smith *et al.*, J. Cryst. Growth **259**, 232 (2003).
[10] T. Walther *et al.*, Phys. Rev. Lett. **86**, 2381 (2001).
[11] J. Stangl *et al.*, Appl. Phys. Lett. **79**, 1474 (2001).
[12] X. Z. Liao *et al.*, J. Appl. Phys. **90**, 2725 (2001).
[13] R. Magalhaes-Paniago *et al.*, Phys. Rev. B **66**, 245312 (2002).
[14] X. Z. Liao *et al.*, Phys. Rev. B **65**, 153306 (2002).
[15] U. Denker, M. Stoffel, and O. G. Schmidt, Phys. Rev. Lett. **90**, 196102 (2003).
[16] A. Malachias *et al.*, Phys. Rev. Lett. **91**, 176101 (2003).
[17] M. Hanke *et al.*, Phys. Rev. B **69**, 075317 (2004).
[18] C. Lang, Mater. Sci. Technol. **19**, 411 (2003).
[19] J. Tersoff, Phys. Rev. Lett. **81**, 3183 (1998).
[20] J. Tersoff *et al.*, Phys. Rev. Lett. **89**, 196104 (2002).
[21] L. L. Shanahan and B. J. Spencer, Interfaces and Free Boundaries **4**, 1 (2002).
[22] B. J. Spencer and J. Tersoff, Phys. Rev. Lett. **79**, 4858 (1997).
[23] B. J. Spencer, P. W. Voorhees, and J. Tersoff, Phys. Rev. B **64**, 235318 (2001).
[24] M. Blanariu and B. J. Spencer, report.
[25] B. J. Spencer, P. W. Voorhees, and S. H. Davis, Phys. Rev. Lett. **67**, 3696 (1991).
[26] D. J. Eaglesham and M. Cerullo, Phys. Rev. Lett. **64**, 1943 (1990).
[27] M. Albrecht, S. Christiansen, and J. Michler, Appl. Phys. Lett. **67**, 1232 (1995).
[28] J. A. Floro *et al.*, Phys. Rev. Lett. **79**, 3946 (1997).
[29] W. Dorsch *et al.*, Appl. Phys. Lett. **72**, 179 (1998).
[30] P. Sutter, P. Zahl, and E. Sutter, Appl. Phys. Lett. **82**, 3454 (2003).
[31] A. Rastelli *et al.*, Phys. Rev. B **68**, 115301 (2003).